TROPICAL HYDROLOGICAL CYCLE STATES REVEALED IN HIRS WATER VAPOR DATA

John J. Bates
NOAA/ERL Climate Diagnostics Center
Boulder, CO 80303 USA

1. HYDROLOGICAL CYCLE CLIMATE RESEARCH

The Earth's atmosphere is unique amongst the known planetary atmospheres in that it possesses a complete hydrological cycle. That is, we find water in its three phases: gaseous, as water vapor; liquid, as cloud liquid water; and solid, as ice and snow. The existence of a complete hydrological cycle on the Earth greatly modifies the climate, making this planet hospitable to a wide variety of life. It, however, also greatly complicates understanding and prediction of climate because the water and energy cycles interact in a non-linear way on all time and space scales. On the shortest time scales, within thunderstorms, the three phases of water can be found at the same time within a vertical column in the atmosphere. On seasonal to interannual time scales, the effects of regional changes in sea surface temperature in the Pacific Ocean are communicated globally by changes in the tropical atmospheric hydrological cycle. On decadal to centennial time scales, differences in precipitation minus evaporation drive the global oceanic thermohaline circulation thought by many to be the Achilles heel of long term climate variability.

2. SATELLITE ERROR CHARACTERISTICS - A KEY ISSUE FOR CLIMATE STUDIES

A variety of methods are required to characterize the errors from any satellite observational system. These include, but are not limited to, forward radiative transfer simulation studies, on-board calibration, vicarious calibration and validation with in situ observations, random and systematic sampling errors, and retrieval errors. A complete discussion of the error characteristics of HIRS water vapor observations can be found in Wu et al. (1993) and Bates et al. (1996). The typical lifetime of a satellite instrument is on the order of 3-5 years. Obtaining a long time series of observations from satellites requires the use of many similar, but slightly different instruments, on many different satellites. Thus, a key issue for the use of satellite data in climate studies is the accurate characterization of instrument errors from one instrument to the next. Bates et al. (1996) have established a method for the intersatellite calibration of NOAA polar-orbiting satellite HIRS/MSU instruments. Figure 1 shows the empirical distribution functions of HIRS channel 12 brightness temperature anomalies for the overlap periods of different NOAA satellites from 1979-1994. There are four lines on each diagram; one for each satellite and one for the ascending and descending passes from each satellite. Generally, there is little difference between the ascending and descending passes from a single instrument, but there are sometimes significant differences between satellites. This suggests that differences in the relative filter response functions between the different satellites are the largest source of discrepancy between the different satellites. To obtain a seamless time series of these observations, all anomaly distributions are adjusted to a baseline instrument. To date, we have only analyzed the NESDIS cloud cleared radiances, but we are now using TOVS 1b data as part of the TOVS Pathfinder program.

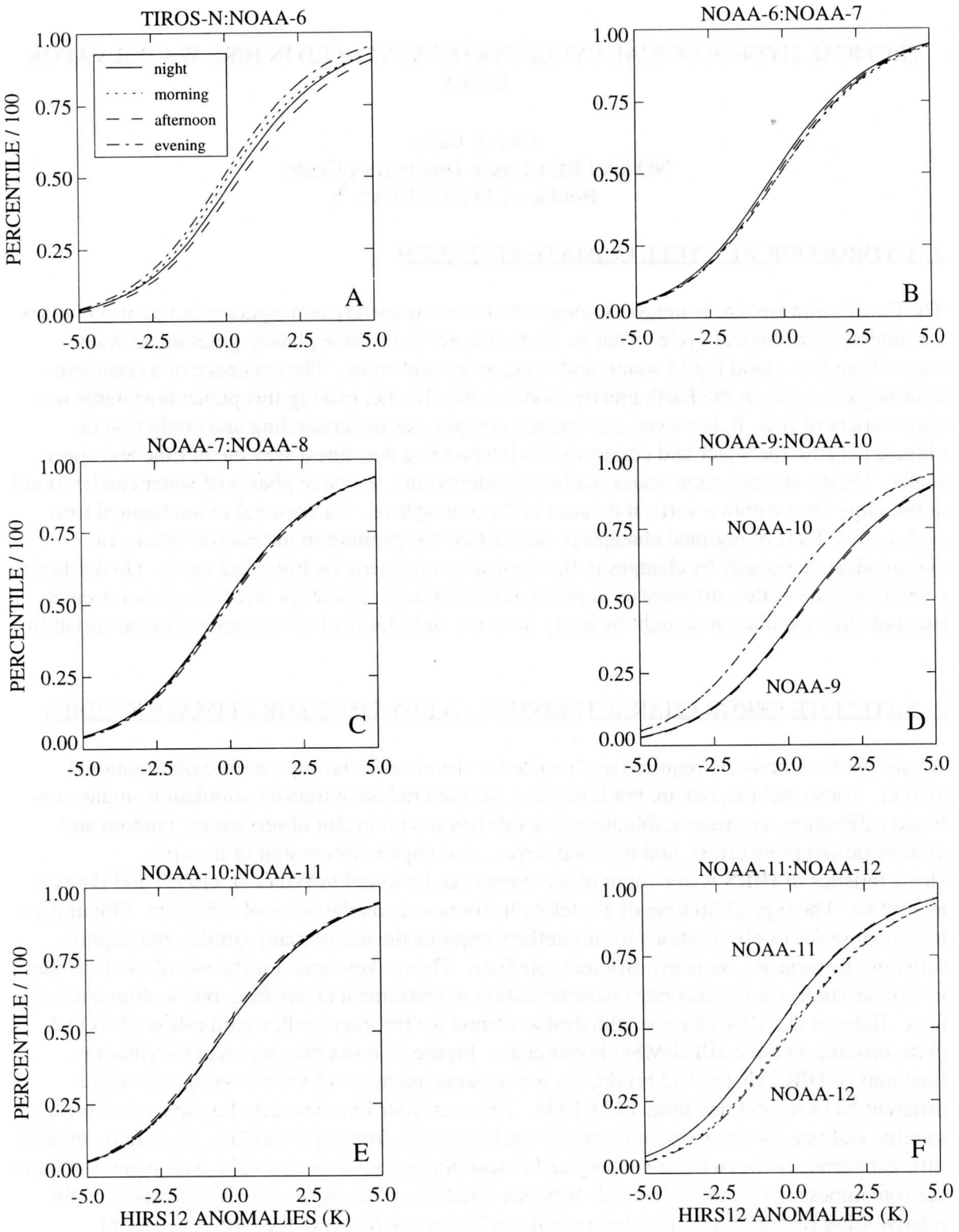

Figure 1: Cumulative EDF for all overlap periods as a function of equatorial crossing time.

3. UPPER TROPOSPHERIC HUMIDITY VERSUS CLEAR SKY OUTGOING LONGWAVE RADIATION

3.1. Seasonal Cycle Observations

Long term seasonal mean maps of the UTH (Bates et al., 1996) and clear sky OLR (CLERA; Slingo et al., 1997) from 60°N-60°S show the largest values of CLERA OLR are found in the tropics (Figure 2). This is where the Earth is losing the largest amount of longwave radiation to space. Within the tropics, there is a very high correlation between the regions of relatively high CLERA OLR and low UTH and vice-versa. Thus, the long term mean clear sky OLR is largely determined by the long term mean UTH.

The UTH is computed using clear sky only brightness temperature observations from the HIRS instrument on the NOAA polar orbiting satellites. The clear sky OLR observations (CLERA) are from the ECMWF Re-Analysis which combines conventional and satellite data. The satellite data uses the same NESDIS clear column radiances as our UTH data, so these two data sets are not independent. Within the Tropics, the lowest (highest) regions of UTH occur in the regions of highest (lowest) clear sky OLR; the descending (ascending) branches of the Hadley and Walker circulations. Generally, the lowest UTH occurs in the winter hemisphere between latitudes 10° and 20°. The patterns of UTH and CLERA OLR undergo a large seasonal cycle associated with the movement and intensification of the global monsoon system.

During the DJF season, maxima in clear sky OLR of 300 Wm^{-2} or greater occur over the subtropical Pacific Ocean southwest of Hawaii, over the Arabian Sea and extending west across North Africa, and over the Caribbean Sea. Somewhat less intense maxima occur in the southern hemisphere over Australia and extending west into the Indian Ocean, over South Africa and extending west into the South Atlantic Ocean, and from the west coast of South America extending northwest into the central Pacific Ocean. There is a similar pattern during the MAM season, although the intensity of the patterns is less during this transitional season. A major change in the pattern of clear sky maxima and minima is apparent in the JJA season. This pattern is dominated by a zonal band of clear sky OLR along 20°S with maxima in the southeast Pacific, southeast Atlantic and southeast Indian Oceans. There is also large maxima in OLR over Saudi Arabia and extending west over North Africa.

3.2. Dynamic Interpretations of the Seasonal Cycle

The traditional explanation of the location and intensity of these subtropical subsidence areas involves the seasonal mean zonally-averaged Hadley cell overturning circulation which shows strong decent in the subtropics. However, it is clear from the UTH seasonal cycle that this concept is not particularly useful since there are very large meridional contrasts in UTH and CLERA OLR. Explaining the observed meridional patterns requires theories about the east-west as well as the north-south overturning circulations in the tropics. In other words, what is the relationship between the intensity and location of the monsoons and subtropical deserts?

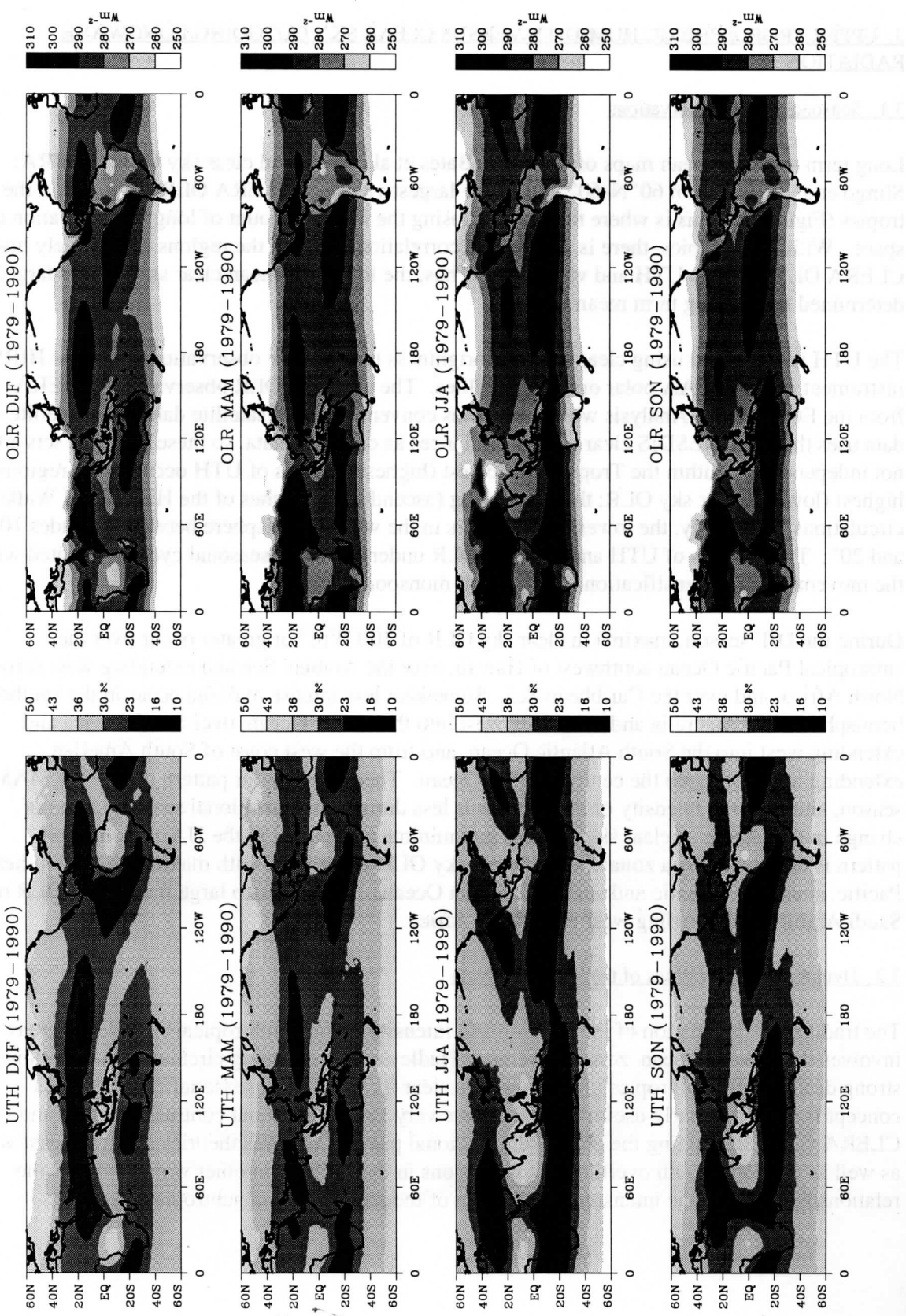

Figure 2: Long-term seasonal mean CLERA OLR and UTH.

Webster has conducted numerous diagnostic and theoretical studies (e.g., Webster and Chou, 1980; Webster and Lau, 1878) of the seasonal evolution of the monsoon-desert system. This research emphasizes the roles of both land-ocean differential heating and the hydrological cycle. Essential features of the observed monsoon system can not be explained without the use of full hydrology.

Another explanation of this maxima in clear sky OLR over Saudi Arabia and North Africa, and perhaps other of the subtropical subsidence regions, has been offered by Rodwell and Hoskins (1996). Their study uses and idealized model that suggests that a coupled monsoon-desert mechanism may be responsible for these subsidence areas whereby remote diabatic heating in the Asian monsoon region can induce a Rossby-wave pattern to the west. This Rossby-wave solution includes a warm thermal structure that interacts with air on the southern flank of the mid-latitude westerlies causing it to descend. They speculate that the monsoon-forced adiabatic descent results in clear air and a local diabatic enhancement of the overturning circulation which effectively doubles the strength. However, a close examination of the figures in this paper reveals that this monsoon-forced adiabatic descent only contributes 1/6th of the observed total. It is hoped that further analysis of the observed UTH data set may lead to improved understanding of the relationships between monsoons and deserts.

3.3. Interannual Variability Observations

Empirical orthogonal function (EOF) analysis was performed separately on the HIRS 12 upper tropospheric humidity (UTH), Reynolds blended SST, all-sky outgoing longwave radiation (OLR), and CLERA monthly mean anomaly datasets. To keep the comparisons uniform, the data were analyzed from 1982-1993 (since the satellite SST data only begin in 1982) for the tropical region 30°N-30°S. In all cases, the first mode is associated with interannual, global variability during ENSO warm events. Because of this, the principle component time series for each dataset has been plotted on a single figure (Figure 3e). The amount of variance explained by the first mode ranges from 12% for the HIRS 12 UTH and CLERA, to 24% for the OLR, and to 32% for the SST.

The spatial patterns of the leading mode for each parameter are shown in Figure 3a-d. The classic ENSO warm event SST signature (Fig. 3a) is evident with positive anomalies in the central and eastern equatorial Pacific and negative anomalies in the western equatorial Pacific extending poleward to the extratropics. This interannual SST EOF pattern has been found in independent analysis of ship-only data and satellite-only data (Bates, 1994). The spatial pattern for OLR anomalies (figure 3b) shows a pattern of near equatorial anomalies that results from the shift of convection from the western Pacific Ocean to the central and eastern Pacific during warm events. There are positive OLR anomalies centered near the dateline and extending into the eastern equatorial Pacific. Negative OLR anomalies are found in the western equatorial Pacific and there is a small negative anomaly over northeastern Brazil.

The spatial pattern of the UTH EOF (Fig. 3c) shows some similar features, but also some distinctly different features when compared to the OLR. Along the equator in the Pacific Ocean, the UTH and OLR features are most similar. At the equator and the dateline, there is a minimum

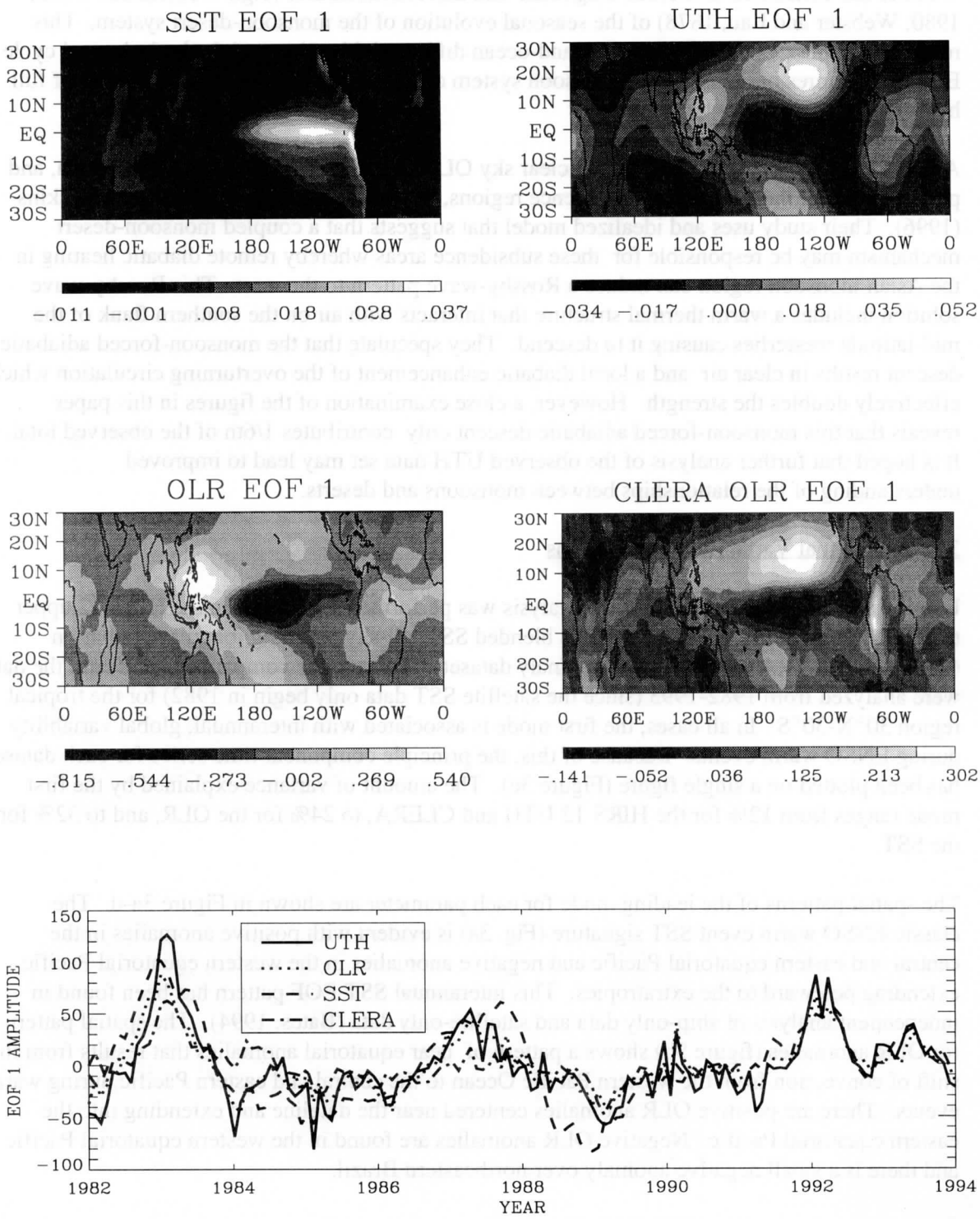

Figure 3: Spatial pattern of the leading mode empirical orthogonal function for anomalies of Reynolds SST,UTH, all-sky OLR and clear-sky CLERA OLR. Also shown is the time series of the leading mode principal component.

in UTH. The minimum extends eastward to a second minimum in the eastern Pacific. Relative maximum along the equator are found in the western Pacific and across South America extending over northeast Brazil. The most striking difference between the UTH and OLR, however, occurs in the subtropical latitudes. A large maximum in UTH is found just southeast of Hawaii. There is only a weak hint of this anomaly in the OLR data. The UTH data also show a series of maximum and minimum across the southern hemisphere subtropics including a minimum from southwestern Australia extending westward towards Madagascar, a maximum to the east of Australia, and two minimum further east one on either side of South America. The CLERA OLR spatial pattern (Figure 3d) is very similar to the UTH, since both use the HIRS channel 12 data. However, the ECMWF re-analysis only used the HIRS 12 data over the ocean. Consequently there are some large differences between the two over the land areas.

An examination of the tropical area average interannual changes (Figure 4) in SST, UTH, and Tropospheric temperature (MSU2), however, shows no significant correlation between UTH and SST and MSU2 time series. The behavior of tropical UTH appears quite different from one ENSO event to the other. During the 1982-83 ENSO the UTH decreases markedly, during the 1986-87 ENSO event the UTH remains about constant, and during the 1991-92 ENSO the UTH increases slightly. The most striking aspect of these time series is the dramatic drop in tropical UTH during the 1982-83 ENSO. This suggests that a negative UTH feedback does exist for certain states of the tropical hydrological cycle. We are continuing our analysis of these data sets and collaborating with GCM model runs to improve our understanding of these variations.

Figure 5 shows the mean and anomalous UTH and CLERA OLR for the DJF season of 1982-83. Large positive and negative anomalies are found over the Pacific Ocean in the Tropics and Subtropics. Positive UTH anomalies of 6-10% are found over the equator from the dateline to the South American coast and negative anomalies of 6-10% are found the norther subtropics between Hawaii and Baja California. However, because the base relative humidity is already low over the subtropics, the CLERA OLR anomaly is 13-20 Wm^{-2} but is only a negative 6-13 Wm^{-2} over the Tropics.

3.4. Dynamic interpretation of interannual variability

The abrupt, large decrease in tropical UTH during the 1982-83 ENSO, and accompanying changes in global precipitation, have gained increased attention given recent advances in our understanding of paleoclimate records. Broeker at al. (1996) present evidence using a variety of paleoclimate indices that during peak glacial time, the tropical water vapor budget was substantially lower than today. They hypothesize a chain of events that suggest that water vapor cycling through the tropical monsoons was a major driver, not just a feedback, of climate change. In this scenario, a causal chain is triggered by reorganizations of the ocean's thermohaline circulation. These reorganizations reduce upwelling in the tropical Pacific and thus reduce the SST temperature gradient across the Pacific basin. This causes large scale changes in the organization of tropical convection and the cycling of water into the tropical upper troposphere leading to a negative upper tropospheric water vapor feedback. Although this scenario is admittedly speculative, there are many similarities to the 1982-83 ENSO event in UTH.

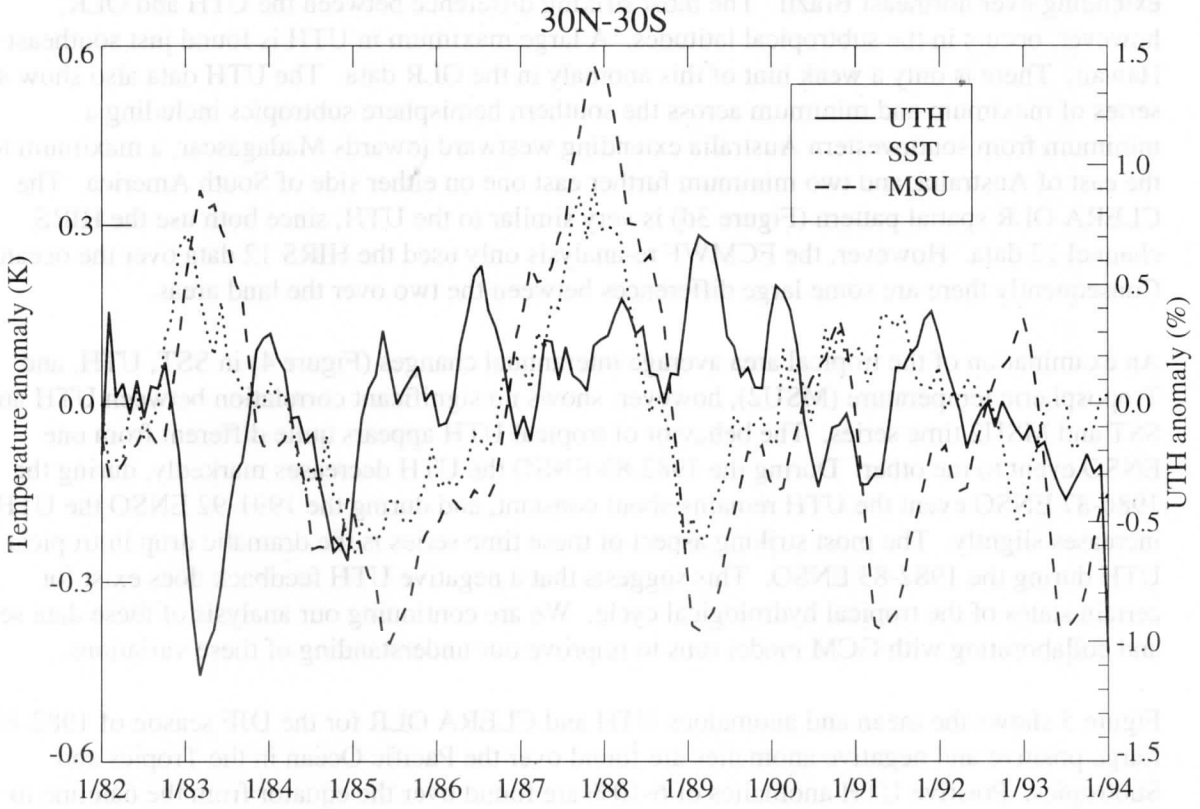

Figure 4: 12-year time series of anomalies of UTH, SST and MSU.

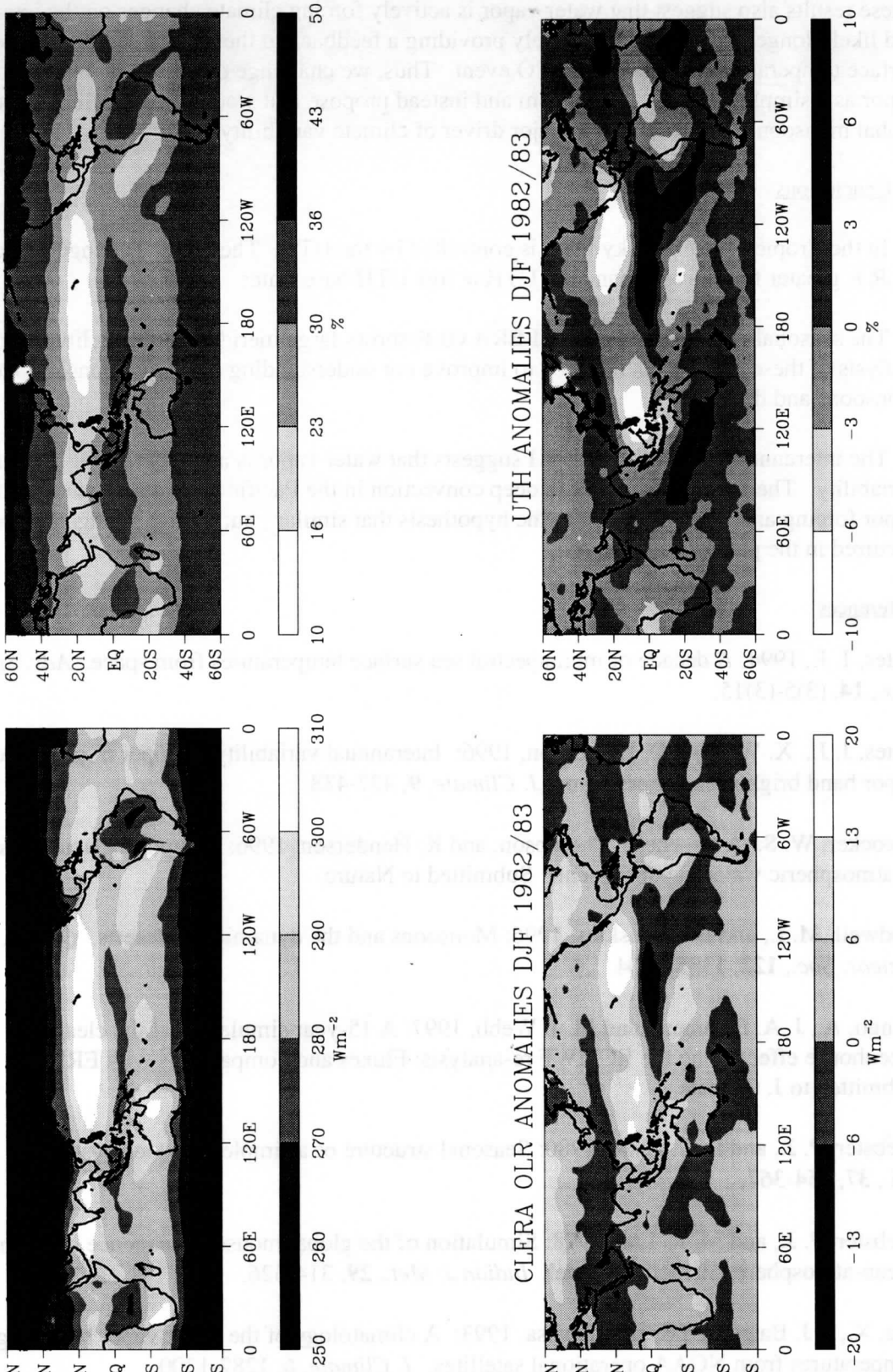

Figure 5: Seasonal mean and anomalous UTH and CLERA OLR for DJF 1982-83.

These results also suggest that water vapor is actively forcing climate changes on the interannual, and likely longer, scales and not merely providing a feedback to the anomalously warm sea surface temperatures during this ENSO event. Thus, we challenge the traditional notion of water vapor as a simple feedback mechanism and instead propose that water vapor cycling through the global monsoon systems can be a major driver of climate variability.

4. Conclusions

1. In the Tropics, the clear sky OLR is controlled by the UTH. The relative change in clear sky OLR is greater for a given change in UTH at low UTH base states.

2. The seasonal cycle of UTH and CLERA OLR shows large meridional variability. Further analysis of these data sets is required to improve our understanding of the relationship between monsoons and deserts.

3. The interannual variability of UTH suggests that water vapor is actively forcing climate variability. The far eastward shift in deep convection in the Pacific lead to a negative water vapor forcing and lends credence to the hypothesis that similar , but more prolonged events, occurred in the paleoclimate record.

References

Bates, J. J., 1994: A decade of multispectral sea surface temperatures from space. *Adv, Space Res.*, **14**, (3)5-(3)15.

Bates, J. J., X. Wu, and D. L. Jackson, 1996: Interannual variability of upper troposphere water vapor band brightness temperature. *J. Climate*, **9**, 427-438.

Breocker, W. S., A Greene, L Thompson, and K. Henderson, 1996: Mountain glaciers: Recorders of atmospheric water vapor content? Submitted to Nature.

Rodwell, M. J., and B. J. Hoskins, 1996: Monsoons and the dynamics of deserts. *Q. J. R. Meteor. Soc.*, **122**, 1385-1404.

Slingo, A., J. A. Pamment, and M. J. Webb, 1997: A 15-year simulation of the clear-sky greenhouse effect using the ECMWF re-analysis: Fluxes and comparisons with ERBE. Submitted to J. Climate.

Webster, P. J., and L. C. Chou, 1980: Seasonal structure of a simple monsoon system. *J. Atmos. Sci.*, **37**, 354-367.

Webster, P. J., and M. K. Lau, 1978: Simulation of the global monsoon sequence by a simple, ocean-atmosphere interaction model. *Indian J. Met.*, **29**, 314-326.

Wu, X., J. J. Bates, and S. J. S. Khalsa, 1993: A climatology of the water vapor band brightness temperatures from NOAA operational satellites. *J. Climate*, **6**, 1282-1300.

TECHNICAL PROCEEDINGS OF

THE NINTH INTERNATIONAL TOVS STUDY CONFERENCE

Igls, Austria

20-26 February 1997

Edited by

J R Eyre

Meteorological Office, Bracknell, U.K.

Published by

European Centre for Medium-range Weather Forecasts
Shinfield Park, Reading, RG2 9AX, U.K.

May 1997